



OPEN ACCESS

Operations Research and Decisions

[www.ord.pwr.edu.pl](http://www.ord.pwr.edu.pl)

OPERATIONS  
RESEARCH  
AND DECISIONS  
QUARTERLY



# Optimising pedestrian flow in a topological network using various pairwise speed-density models

Ruzelan Khalid<sup>1\*</sup> Mohd Kamal Mohd Nawawi<sup>1</sup> Nurhanis Ishak<sup>2</sup> Md Azizul Baten<sup>3</sup>

<sup>1</sup>*Institute of Strategic Industrial Decision-Modelling (ISIDM), School of Quantitative Sciences, University Utara Malaysia, 06010 UUM Sintok, Kedah, Malaysia*

<sup>2</sup>*Faculty of Management and Information Technology, University Islam Sultan Azlan Shah, 33000 Kuala Kangsar, Perak, Malaysia*

<sup>3</sup>*Department of Statistics, School of Physical Sciences, Shahjalal University of Science and Technology, Sylhet-3114, Bangladesh*

\*Corresponding author, email address: [ruzelan@uum.edu.my](mailto:ruzelan@uum.edu.my)

## Abstract

A speed-density model can be utilised to efficiently flow pedestrians in a network. However, how each model measures and optimises the performance of the network is rarely reported. Thus, this paper analyses and optimises the flow in a topological network using various speed-density models. Each model was first used to obtain the optimal arrival rates to all individual networks. The optimal value of each network was then set as a flow constraint in a network flow model. The network flow model was solved to find the optimal arrival rates to the source networks. The optimal values were then used to measure their effects on the performance of each available network. The performance results of the model were then compared with that of other speed-density models. The analysis of the results can help decision-makers understand how arrival rates propagate through traffic and determine the level of the network throughputs.

**Keywords:** *topological network, speed-density models, optimal arrival rates, network flow model, pedestrian flow*

## 1. Introduction

A transportation problem deals with the best strategy to distribute items from several sources to several sinks or destinations. Each source (e.g., a factory) typically has a capacity of supply, while each destination (e.g., a warehouse) has a requirement of demand. Using the supply and demand information, the transportation cost per unit item from the sources to the destinations is minimized. This problem can be solved using a specialized algorithm or a linear program [11, 31]. Similarly, a linear program can also be formulated to efficiently flow pedestrians from several sources to several destinations in a topological network.

Analysing and optimising pedestrian flow can help decision-makers provide effective solutions for planning and managing pedestrian movement and paths in public buildings and spaces, such as shopping

malls, sport stadiums, railway stations and airport terminals. Optimising the flow requires us to study the characteristics of pedestrian movement in each available network. This type of study is important to understand how a shockwave (a discontinuity or an interruption) propagates through the traffic flow and to measure the level of service determining how well a transportation facility is operating [27, 33]. In real life, the study and analysis can assist us in identifying potential bottlenecks in particular areas of networks or testing the impacts of potential operational evacuation strategies. The strategies can then be used for planning relevant actions during emergency cases or properly designing buildings or facilities before real construction take place.

Flowing pedestrians through a topological network should consider various factors affecting their flow, e.g., the number of pedestrians moving in a unit of time, density, speed, space size and different routing patterns. The speed of pedestrians, which is the inverse of their density, was first established in 1937 [22]. Other literature reviews, e.g., [7, 10, 18–20], also show that the average speed of pedestrians through a constrained space, either unidirectional or bidirectional movement, is determined by their density in the space. The relationship between the density and speed describing the average behavior of pedestrians moving through space has also been modelled and analysed based on a secondary dataset of pedestrian speed. The plotted figures show the relationship between density and speed to be nonlinear. Examples of models based on a nonlinear speed-density relationship include the *M/G/C/C* [14, 15, 24, 25, 30], Underwood [29] and Greenberg [8] models.

The density of pedestrians in a topological network can practically be controlled by routing them to relevant downstream and sink networks. To avoid under-utilization or over-utilization of the networks, the density can further be controlled by regulating the pedestrians' arrival rates to the source networks using available speed-density models. By adjusting these two variables, the flow in all networks can be optimised. However, how each speed-density model analyses and optimises the performance of a topological network, especially in terms of its throughput, has rarely been reported. Thus, this paper analyses and optimises the performance of a topological network using various speed-density models. The performance was optimised by deriving the optimal arrival rates of pedestrians to all source networks and appropriately channelling their movement paths to downstream networks. The generated results can help decision-makers understand the impacts of arrival rates on traffic flow, compare the network performance using various speed-density models and justify the appropriate actions to best flow pedestrians out of a facility.

This paper extends the work of Khalid et al. [16] where some speed-density models have been used to verify strategies to flow pedestrians in a facility. However, they did not derive the mathematical forms that optimise the density and flow of various speed-density models. Additionally, they did not discuss some of the properties of the speed-density models. The paper is divided into several sections. Section 2 briefly reviews literature related to speed-density models and explains their properties and shortcomings. Taking a speed model as an example, Section 3 derives its optimal density and flow. The speed-density and flow-density relationships of various speed-density models are then plotted. This section also describes how to measure the performance of a constrained space and optimise the throughput of a topological network using the speed-density models and network flow programming. Based on the methodology, Section 4 analyses the performance of a topological network, considering a university hall as a case study. Section 5 discusses the limitations of this study based on different assumptions. Section 6 concludes the paper.

## 2. Literature review

The speed and density relationship in a constrained space has long been modelled. The well-known relation in the traffic flow theory,  $q = \rho v$ , where  $q$  is flow,  $\rho$  density and  $v$  speed was verified by a study conducted by Predtechenskii and Milinskii between 1946 and 1948 [22]. The study also established a graphical approach to studying pedestrian traffic flow in time–space diagrams. The relationship among flow, speed and density of pedestrian flow in selected facilities, considering the socio-economic situations of certain countries, has also been available. For example, Hankin and Wright [10] and Oeding [19] considered uni-directional pedestrian flow, while Older [20], Navin and Wheeler [18], and Fruin [7] considered bi-directional or mixed pedestrian flow in relevant facilities.

**Table 1.** Various pairwise speed-density models

Model	Function	Optimal $\rho$	Optimal $q$
Greenshields [8]	$v(\rho) = v_f \left(1 - \frac{\rho}{\rho_m}\right)$	$\rho_{\text{opt}} = \frac{\rho_m}{2}$	$q_{\text{opt}} = \frac{v_f \rho_m}{4}$
Greenberg [7]	$v(\rho) = v_f \ln \frac{\rho_m}{\rho}$	$\rho_{\text{opt}} = \frac{\rho_m}{e}$	$q_{\text{opt}} = \frac{v_f \rho_m}{e} \ln e$
Underwood [29]	$v(\rho) = v_f e^{-\frac{\rho}{\rho_m}}$	$\rho_{\text{opt}} = \rho_m$	$q_{\text{opt}} = \frac{v_f \rho_m}{e}$
Drake /Northwestern [3]	$v(\rho) = v_f e^{-\frac{1}{2} \left(\frac{\rho}{\rho_m}\right)^2}$	$\rho_{\text{opt}} = \rho_m$	$q_{\text{opt}} = \frac{v_f \rho_m}{e^{\frac{1}{2}}}$
Pipes–Munjal [20]	$v(\rho) = v_f \left(1 - \left(\frac{\rho}{\rho_m}\right)^n\right)$	$\rho_{\text{opt}} = \left(\frac{\rho_m^n}{n+1}\right)^{\frac{1}{n}}$	$q_{\text{opt}} = \left(\frac{n}{n+1}\right) v_f \left(\frac{\rho_m^n}{n+1}\right)^{\frac{1}{n}}$
Drew [4]	$v(\rho) = v_f \left(1 - \left(\frac{\rho}{\rho_m}\right)^{n+\frac{1}{2}}\right)$	$\rho_{\text{opt}} = \left(\frac{2\rho_m^{n+\frac{1}{2}}}{2n+3}\right)^{\frac{2}{2n+1}}$	$q_{\text{opt}} = v_f \left(\frac{2\rho_m^{n+\frac{1}{2}}}{2n+3}\right)^{\frac{2}{2n+1}} \left(\frac{2n+1}{2n+3}\right)$
M/G/C/C linear [2]	$v(\rho) = \frac{v_f}{\rho_m}(\rho_m + 1 - \rho)$	$\rho_{\text{opt}} = \frac{\rho_m + 1}{2}$	$q_{\text{opt}} = \frac{v_f}{4\rho_m}(\rho_m + 1)^2$

The first pairwise speed-density model was developed by Greenshields [9] based on the data collected in a lane of a two-way rural road. He simply associated speed and density as a linear relationship (see Table 1), where speed approaches free flow speed,  $v_f$  when density,  $\rho$  approaches zero. Since the linear relationship is hardly found in many real-world processes, the validity of the model is, however, questionable. As a result, nonlinear speed-density models were then proposed.

The first nonlinear speed-density model was developed by Greenberg [8]. He related the decrement of speed as density increases using a logarithmic function. However, the speed in the model increases to infinity when the density approaches zero. As a result, the model cannot predict speed at lower densities. To overcome the limitation, Underwood [29] developed an exponential speed-density model. However, the speed in this model becomes zero only when the density reaches infinity. Thus, the model cannot be used to predict speed at high densities.

To cater for the problem, other models for modelling a speed-density relationship were then proposed. They include Drake (also known as the Northwestern) [4], Pipes–Munjal [21] and Drew [5] models. The Pipe–Munjal and Drew models are basically varied versions of the Greenshields model. Thus, they still

inherit the Greenshields model's shortcomings (cf. Table 1). The Greenberg model is undefined when the density is zero since the speed approaches infinity when the density approaches zero.

A speed-density model relationship was also modelled by Yuhaski and Smith [34] through their *M/G/C/C* linear (Table 1) and exponential models. The exponential model is given as follows:

$$V_n = V_f \exp \left( - \left( \frac{n-1}{\beta} \right)^\gamma \right) \quad (1)$$

where

$$\beta = \frac{a-1}{\left( \ln \left( \frac{V_f}{V_a} \right) \right)^{1/\gamma}} = \frac{b-1}{\left( \ln \left( \frac{V_f}{V_b} \right) \right)^{1/\gamma}}, \quad \gamma = \frac{\ln \frac{V_a}{V_f}}{\ln \frac{a-1}{b-1}}$$

where  $\gamma, \beta$  are the shape and scale parameters for the exponential model, respectively,  $V_n$  – walking speed for  $n$  pedestrians in a space,  $V_a$  – walking speed when the density is 2 pedestrians/m<sup>2</sup> (0.64 m/s),  $V_b$  – walking speed when density is 4 pedestrians/m<sup>2</sup> (0.25 m/s),  $V_f$  – walking speed for a single pedestrian (1.5 m/s),  $n$  – number of pedestrians in a space,  $a = 2lw, b = 4lw, c = 5lw, l, m, m$  – space length, and width, respectively.

As in the Greenberg model, the *M/G/C/C* exponential is also undefined for  $n < 1$ . This can be shown as follows. Notice that  $\ln \left( \frac{a-1}{b-1} \right)$  is only defined if  $Z = \frac{a-1}{b-1} = \frac{2lw-1}{4lw-1} > 0$ . Since  $lw > 0$ , then  $lw = \frac{Z-1}{4Z-2} > 0$ . To satisfy this inequality, the values of  $Z$  must either be  $0 < Z < 0.5$  or  $Z > 1$ .  $Z > 1$  occurs only when  $0 < lw < 0.25$ , which is for a very small space size,  $lw$ . For these values of  $lw$ ,  $\gamma = \{\gamma : \gamma > 0\}$ .  $0 < Z < 0.5$  occurs when  $lw > 0.25$ . This means that when a space is getting bigger (i.e.,  $lw \rightarrow \infty$ ),  $Z \rightarrow 0.5$ .  $0 < Z < 0.5$  yields

$$\gamma = \left( \gamma : 0 < \gamma < \ln \frac{\ln \frac{V_a}{V_f}}{\ln \frac{V_b}{V_f}} \times \frac{1}{\ln 0.5} \right) = \{\gamma : 0 < \gamma < 1.0729\}$$

Since the values of  $\gamma$  are restricted in this range and  $\beta < 0$ ,  $\left( \frac{n-1}{\beta} \right)^\gamma$  is undefined for  $n < 1$ . This is the reason why  $V_n$  is undefined for  $n < 1$  (cf. Figure 2).

All the models are called a single regime since a single function is used to model free flow and density. To improve such an over-simplified relationship, multi-regime models, providing different equations for free flow and congested regimes under different conditions, have been proposed. Examples of multi-regime models include the Edie model [6] and two- and three-regime models [17]. Since multi-regime models are complex and difficult to apply, this paper only employs single-regime traffic speed-density models to analyse and optimize pedestrian flow through a topological network.

### 3. Materials and method

#### 3.1. Method

Figure 1 shows the method for measuring the performance of a topological network and optimising its throughput using speed-density models and a network flow model. In brief, this study first collected and reviewed available speed-density models to understand their properties and derive their optimal densities and flow. Using a particular speed-density model, the optimal arrival rates for all the individual networks in a topological network were derived. Each of these optimal arrival rates was then set as a flow constraint in a network flow model. The objective function of the network flow model is to optimise the flow in all the networks.

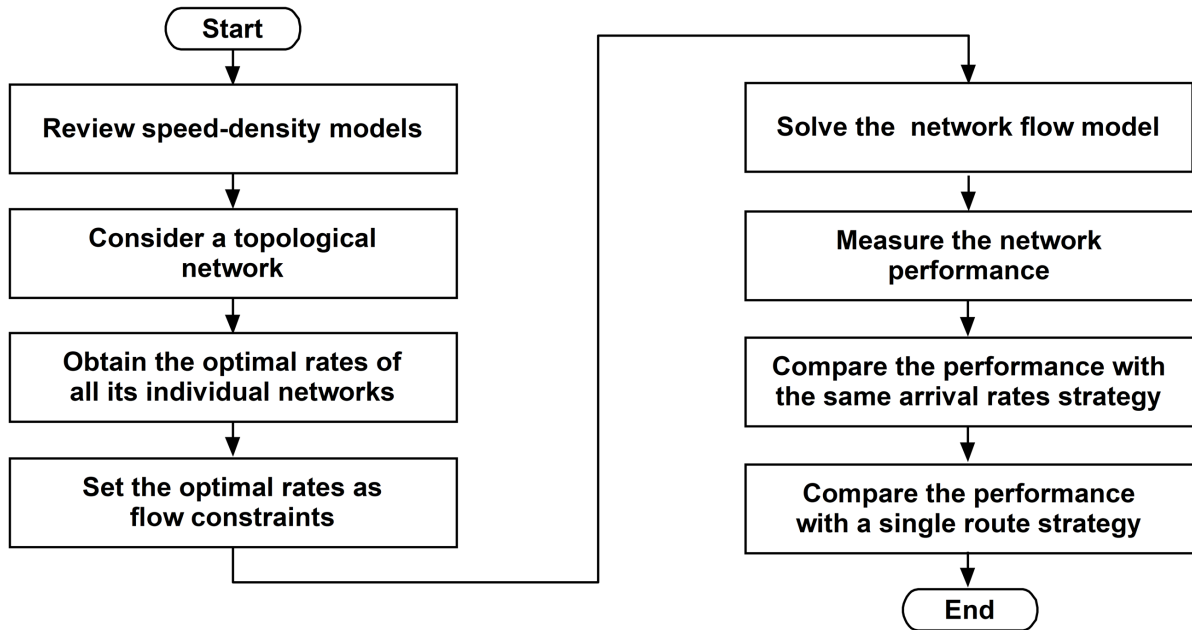


Figure 1. The methodology of the study

The model was then solved using linear programming software to obtain the optimal arrival rates to the source networks. The optimal arrival rates were used to measure its effect on the performance of each of the available networks, especially in terms of its throughput and blocking probability. The performance results were then compared with the performance results generated when the same arrival rates were imposed on all source corridors and when the shortest route policy was implemented in the topological network.

#### 3.2. Deriving the optimal density and flow of a speed-density model

Based on a speed-density model, its optimal density and flow can be derived. For example, the Underwood model relates the speed-density as

$$v(\rho) = v_f e^{-\frac{\rho}{\rho_m}} \quad (2)$$

where  $v$  is the average traffic speed,  $v_f$  is the free flow (maximum) speed (the speed of a single pedestrian or vehicle),  $\rho$  is the traffic density (the number of pedestrians or vehicles per unit area) and  $\rho_m$  is the

maximum (critical) density at which a traffic jam occurs and the speed is near to zero. Any increase in traffic density will decrease the average flow speed in a space (e.g., a corridor or a road). This decreasing rate may differ for different populations. In the case of pedestrian population, the density is the number of pedestrians divided by the area of space (i.e., the product of its length and width). The number of pedestrians is thus expressed in their density in a  $1 \text{ m}^2$  space. For example, consider a space of  $10 \times 3 \text{ m}^2$  in which the current number of pedestrians is 60. The traffic density (in pedestrians per second, i.e., peds/s) for the space can then be calculated as  $\rho = 60/(10 \times 3) = 2$ . If we further consider that  $v_f = 1.5 \text{ m/s}$  and  $\rho_m = 5 \text{ peds/m}^2$ , the current speed of the pedestrians is  $v(2) = 1.5e^{-0.4} = 1.00548 \text{ m/s}$ . Using the same approach, if there are 120 pedestrians,  $\rho = \frac{120}{10 \times 3} = 4 \text{ peds/m}^2$  and  $v(4) = 1.5e^{-0.4} = 0.67399 \text{ m/s}$ . The pedestrian flow through the space,  $q$ , is given by

$$q = \rho v = \rho v_f e^{-\frac{\rho}{\rho_m}} \quad (3)$$

The pedestrian flow refers to the number of pedestrians crossing a section of a space in a unit of time. The usual unit for flow is peds/m/s (pedestrians per meter width per second). Thus, the pedestrian flow  $q$  through the  $10 \times 3 \text{ m}^2$  space with 60 pedestrians is  $2 \times 1.5e^{-0.4} = 2.01096 \text{ peds/m/s}$ , while with 120 pedestrians it is  $2.69596 \text{ peds/m/s}$ .

To get the density for the minimum or maximum flow, we find  $\frac{dq}{d\rho}$ , and then set it 0. Taking  $u = \rho v_f$  and  $v = e^{-\frac{\rho}{\rho_m}}$  and using the quotient rule [26], we obtain

$$\begin{aligned} \frac{dq}{d\rho} &= v_f e^{-\frac{\rho}{\rho_m}} - \frac{\rho v_f e^{-\frac{\rho}{\rho_m}}}{\rho_m} = 0 \\ 1 - \frac{\rho}{\rho_m} &= 0 \\ \rho &= \rho_m \end{aligned} \quad (4)$$

To show that  $\rho = \rho_m$  maximizes the flow, we have to find  $\frac{d^2q}{d\rho^2}$ , and check its value

$$\frac{d^2q}{d\rho^2} = -\frac{v_f}{\rho_m} e^{-\frac{\rho}{\rho_m}} - \frac{1}{\rho_m} \left( v_f e^{-\frac{\rho}{\rho_m}} - \frac{\rho v_f e^{-\frac{\rho}{\rho_m}}}{\rho_m} \right)$$

$$\frac{d^2q}{d\rho^2} = \frac{v_f}{\rho_m} e^{-\frac{\rho}{\rho_m}} \left( -2 + \frac{\rho}{\rho_m} \right)$$

Since  $\frac{\rho}{\rho_m} \leq 1$  and  $\frac{v_f}{\rho_m} e^{-\frac{\rho}{\rho_m}} > 0$ , then  $\frac{d^2q}{d\rho^2} < 0$ . The value of  $\frac{d^2q}{d\rho^2} < 0 \forall \rho$  proves that  $q$  is maximized at  $\rho = \rho_m$ . To get the optimal flow,  $q_{\text{opt}}$ , for the Underwood model, we substitute  $\rho = \rho_m$  to equation (3)

$$q_{\text{opt}} = \rho_m v_f e^{-\frac{\rho_m}{\rho_m}} = \rho_m v_f e^{-1} = \frac{\rho_m v_f}{e} \quad (5)$$

Thus, the optimal flow for the  $10 \times 3 \text{ m}^2$  space is  $q_{\text{opt}} = \frac{5 \times 1.5}{e} = 2.7591 \text{ peds/m/s}$ .

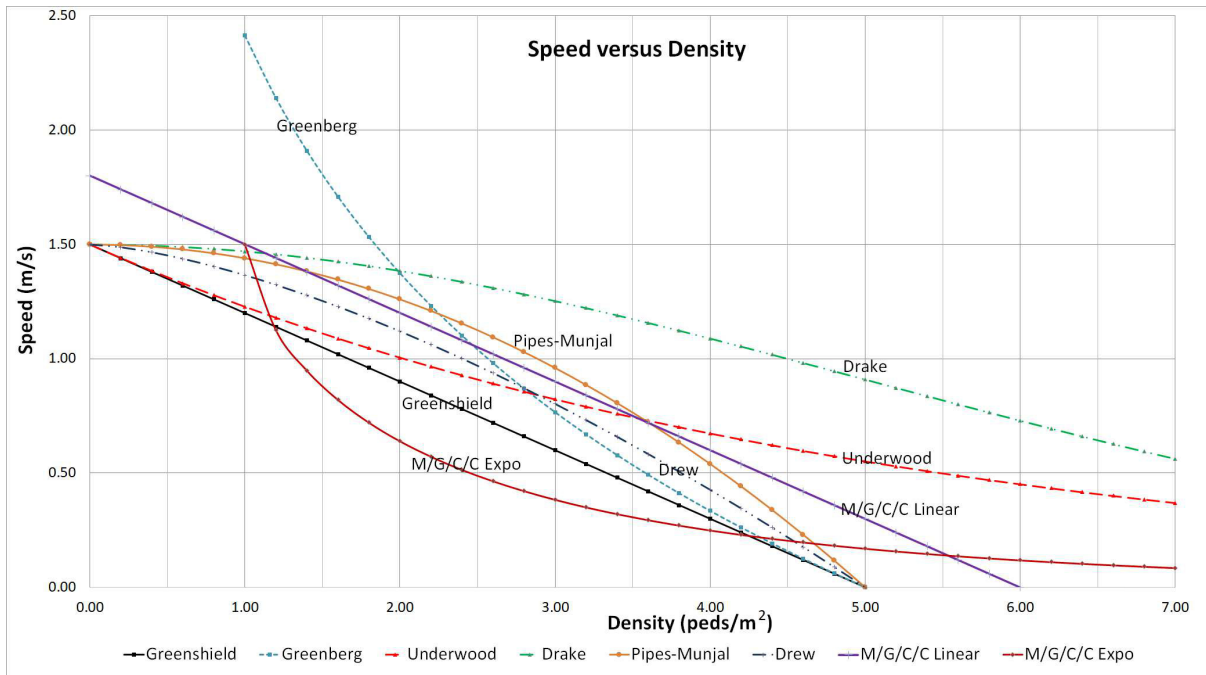


**Figure 2.** Graphical speed-density relationships

Using the same approach, the optimal density and flow for the other speed-density models can be derived. The equation, the optimal density and the flow for each of the speed-density models are given in Table 1. The graphical speed-density relationships for the models are plotted in Figure 2. Based on the plot, the speed of Greenberg and *M/G/C/C* exponential models approaches infinity when the density approaches zero causing the models undefined when the density is zero.

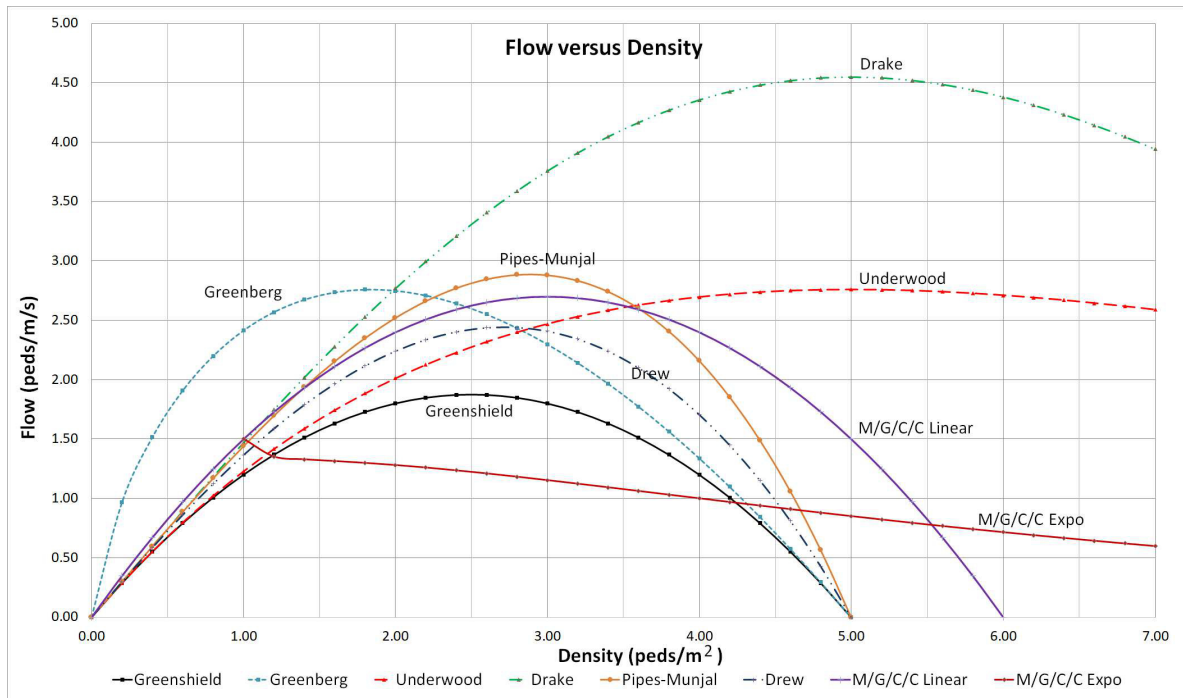


**Figure 3.** Graphical flow-density relationships

The flow-density relationships for the models are shown in Figure 3. The flow is initially zero since the density is zero, i.e., no pedestrians are in a space. The density then continually increases which also



increases the flow until it reaches a relevant point of density maximizing the flow. After this optimal density, any increase in the density will decrease the flow until the flow becomes zero at a critical density, called jam density. At this stage, no movement of pedestrians can be seen.

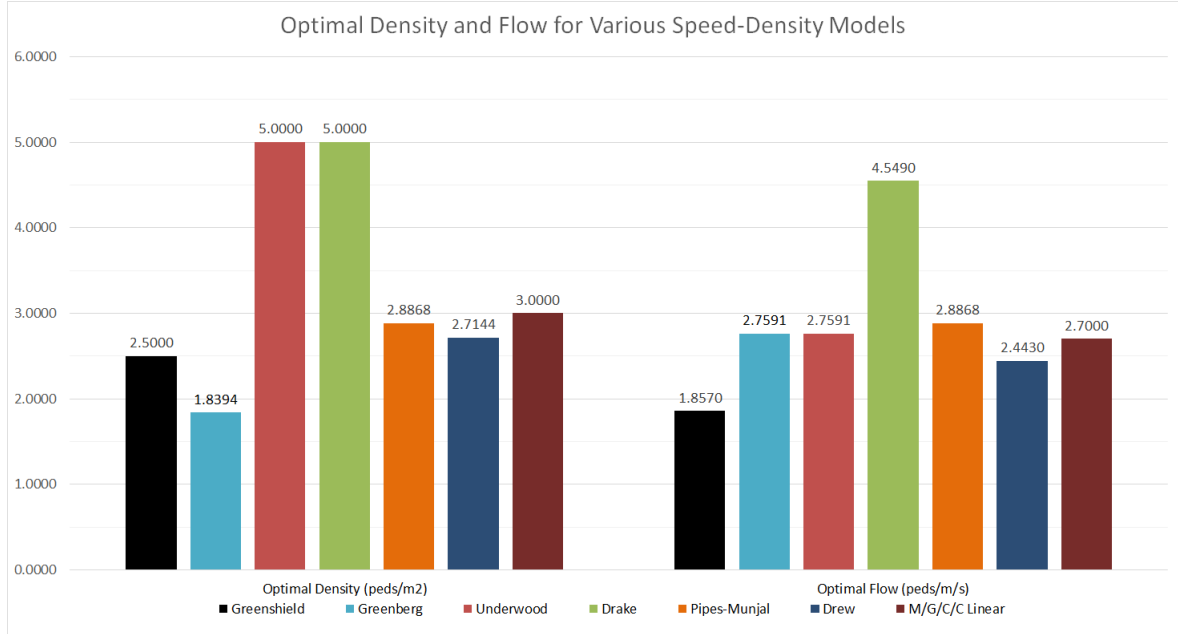


**Figure 4.** The values of the optimal density and flow

The optimal density and flow values for each model are shown in Figure 4. Note that the values of the optimal density and flow for the Pipes–Munjial and Drew models are based on  $n = 2$  and  $n = 1$ , respectively. The value of  $n$  is set arbitrarily to provide a sample of the shape of each of the speed-density and flow-density curves and to derive the optimal density and flow. The scalar parameter  $n$  is the shape parameter describing how the speed-density curves are stretched out over the whole density range [3].

### 3.3. Measuring the performance of a constrained space

The speed and flow of pedestrians in a constrained space are dependent on their density. This density can be managed by controlling the pedestrians' arrival rate to the space. Using the arrival rate, various performances of the space, e.g., its throughput and blocking probability, can be measured. The following equation for blocking probabilities was developed by Yuhaski and Smith [34]:

$$P_n = \frac{(\lambda E(S))^n}{n! f(n) f(n-1) \dots f(2) f(1)} P_0, \quad n = 1, 2, 3, \dots, c \quad (6)$$

where

$$P_0^{-1} = 1 + \sum_{n=1}^c \frac{(\lambda E(S))^n}{n! f(n) f(n-1) \dots f(2) f(1)}$$

$P_n$  is the probability when there are  $n$  pedestrians in the space,  $\lambda$  is the arrival rate to constrained space,  $E(S)$  is the expected service time of a single pedestrian in the space,  $P_0$  is the probability when no pedestrians are present in the space, and  $f(n) = \frac{V_n}{V_f}$  is the service rate, and  $c$  is the capacity of the space. A full-capacity space will block any incoming pedestrians. The probability of such blocking ( $P_{\text{balk}}$ )



equals  $P_n$  where  $n$  equals  $c$ . Based on the equation, Cheah and Smith [2] developed various performance measures of the space which can be computed as:

$$\theta = \lambda(1 - P_{\text{balk}}), \quad E(N) = \sum_{n=1}^c nP_n \quad \text{and} \quad E(T) = \frac{E(N)}{\theta} \quad (7)$$

$\theta$  is the throughput of the space, peds/s,  $E(N)$  is the expected number of pedestrians in the space, peds/s, and  $E(T)$  is the expected service time, s.

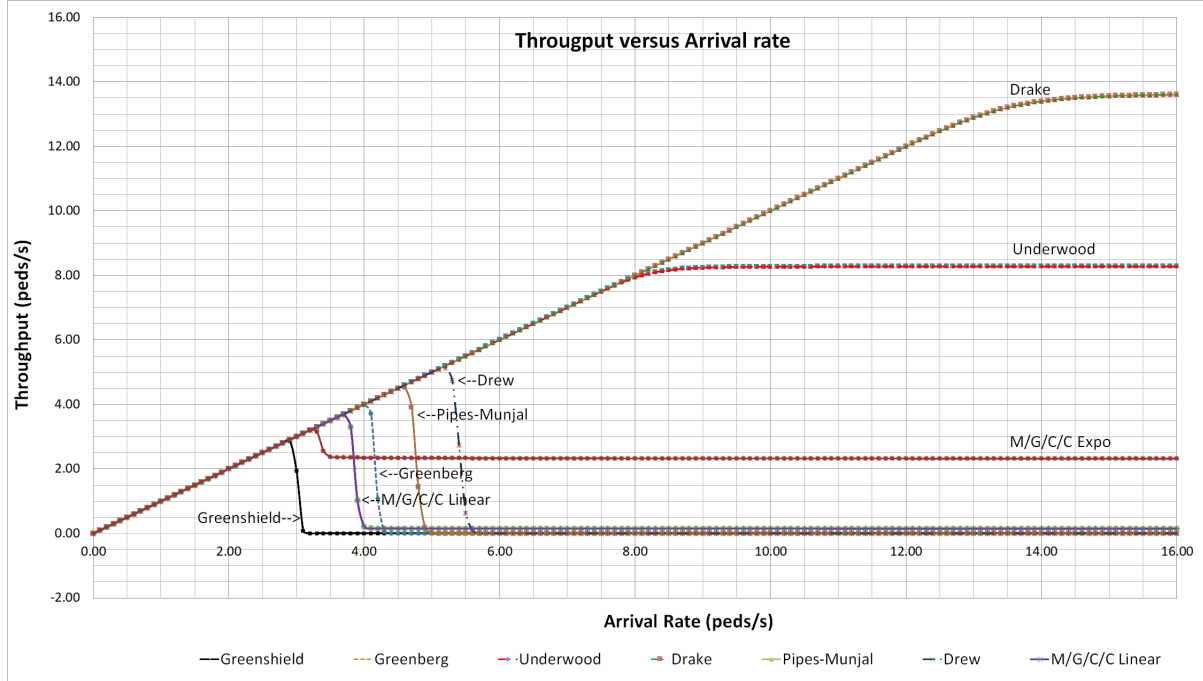


**Figure 5.** Throughput versus arrival rate for various models

The throughputs of a  $10 \times 3 \text{ m}^2$  space based on a series of arrival rates for various speed-density models are plotted in Figure 5. The throughput for each speed-density model initially increases with the increase of its arrival rate, then the throughput reaches its maximum point. Then, the throughput is no longer improved and starts to decrease because the blockage is now being established. The throughput of a space can be optimized by finding its optimal arrival rate. The equation which finds the optimal  $\lambda$ ,  $\lambda_{\text{opt}}$  is given by [13]:

$$\lambda_{\text{opt}} = \left( \frac{(P_0^{-1})^2}{\frac{(\lambda E(S))^c}{c! f(c) f(c-1) \dots f(2) f(1)} \left( (c+1)(P_0^{-1}) - \sum_{i=1}^c \left( \frac{i (\lambda E(S))^i}{i! f(i) f(i-1) \dots f(2) f(1)} \right) \right)} \right)^{1/c} \quad (8)$$

Equation (8) can be used to obtain the optimal arrival rate to a space based on whatever speed-density model since it incorporates  $f(n) = \frac{V_n}{V_f}$ , i.e., the service rate given by the ratio of the average walking speed for  $n$  pedestrians in the space over its average walking speed for a single pedestrian. The optimal  $\lambda$  and its effects on the performance measures for  $10 \times 3 \text{ m}^2$  is shown in Table 2.

**Table 2.** Optimal  $\lambda$  and its effects on the performance measures for a  $10 \times 3 \text{ m}^2$  space

Model	$\lambda$	$\theta$	$P_C$	$E(N)$	$E(T)$
Greenshields [8]	2.9011	2.8782	0.0079	24.0813	8.3667
<i>M/G/C/C</i> exponential [2]	3.2513	3.2219	0.0090	40.3966	12.5380
<i>M/G/C/C</i> linear [2]	3.7082	3.6769	0.0084	32.3958	8.8106
Greenberg [7]	4.0231	3.9943	0.0072	11.3167	2.8332
Pipes–Munjial [20] ( $n = 2$ )	4.5753	4.5365	0.0085	33.1325	7.3035
Drew [4] ( $n = 1$ )	5.1810	5.1357	0.0087	36.6559	7.1375
Underwood [29]	9.3470	8.2555	0.1168	142.7203	17.2879
Drake/Northwestern [3]	15.6341	13.5953	0.1304	143.6363	10.5652

### 3.4. Optimising the throughput of a topological network

A number of connected spaces will form a topological network. The network's throughput can be optimized by setting the optimal arrival rate of each available space as a flow constraint in a network flow model [12]. The mathematical formulation of a network flow model [1, 13, 16, 32] is given as:

Maximize  $x_{T \rightarrow S}$ : flow from super-sink node  $T$  back to super-source node  $S$

subject to:

$$\sum_j x_{i \rightarrow j} - \left( \sum_i x_{j \rightarrow i} - x_{T \rightarrow S} \right) = 0: \text{outflow of node } i \text{ equals its inflow for node } i = S$$

$$\sum_j x_{i \rightarrow j} - \left( \sum_i x_{j \rightarrow i} - x_{S \rightarrow i} \right) = 0: \text{outflow of source node } i \text{ equals its inflow for every node } i \neq s, t$$

$$\sum_j x_{i \rightarrow j} - \sum_i x_{j \rightarrow i} = 0: \text{outflow of node } i \text{ equals its inflow for every node } i \neq s, t$$

$$\left( \sum_j x_{i \rightarrow j} + x_{i \rightarrow T} \right) - \sum_i x_{j \rightarrow i} = 0: \text{outflow of sink node } i$$

$$\left( \sum_j x_{i \rightarrow j} + x_{T \rightarrow S} \right) - \sum_i x_{j \rightarrow i} = 0: \text{outflow of node } i \text{ equals its inflow for node } i = T$$

$$\sum_i x_{i \rightarrow j} \leq c_j: \text{flow capacity for every edge } i \rightarrow j \text{ is smaller or equal to the optimal arrival rate to node } j$$

$$x_{i \rightarrow j} \geq 0: \text{minimum flow for every edge } i \rightarrow j$$

where  $i$  is an index for origin node (vertex)  $i$ ,  $j$  is an index for destination node  $j$ ,  $x_{i \rightarrow j}$  is the flow from origin node  $i$  to destination node  $j$ .

A node represents a space, while an edge represents the link between two spaces. Since there may be a number of source ( $s_1, s_2, \dots, s_n$ ) and sink ( $t_1, t_2, \dots, t_n$ ) spaces in the network, a fictitious super-source  $S$  and a fictitious super-sink  $T$  should be introduced.

The network flow model will generate the optimal arrival rates to the source spaces. These arrival rates will then be used to measure their impacts on all the downstream spaces in terms of their throughputs, blocking probabilities, the expected number of pedestrians and the expected service time.

## 4. Results and discussion

### 4.1. A university hall as a case study

As a case study, we used a university hall [13]. Its structure in terms of available corridors (constrained spaces) is presented in Figure 6.

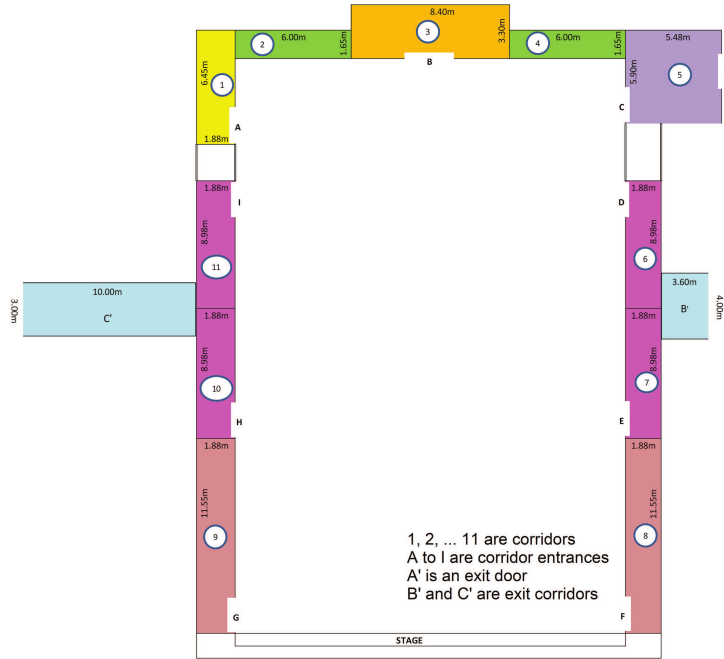


**Figure 6.** The structures of a considered hall

**Table 3.** Dimensions [m] and the optimal arrival rates based on speed-density models

No.	Dimensions		Optimal arrival rate, $\lambda_{opt}$							
	Length	Width	$M/G/C/C$ expo	[8]	[7]	[29]	[3]	[20]	[4]	$M/G/C/C$ linear
1	6.45	1.88	1.9972	1.3897	1.9604	6.7352	11.4096	2.1588	2.4289	2.4393
2	6.00	1.65	1.7633	1.0754	1.5241	6.0861	10.3516	1.6634	1.8683	2.1384
3	8.40	3.30	3.5565	3.1746	4.4074	10.4553	17.5016	5.0019	5.6615	4.1255
4	6.00	1.65	1.7633	1.0754	1.5241	6.0861	10.351	1.6634	1.8683	2.1384
5	5.48	5.90	4.1237	3.4274	4.7818	12.5132	21.0195	5.3767	6.0745	4.8180
6	8.98	1.88	2.0188	1.5607	2.1869	6.3051	10.6251	2.4389	2.7509	2.3729
7	8.98	1.88	2.0188	1.5607	2.1869	6.3051	10.6251	2.4389	2.7509	2.3729
8	11.55	1.88	2.0179	1.7057	2.3781	6.1338	10.2983	2.6775	3.0257	2.3700
9	11.55	1.88	2.0179	1.7057	2.3781	6.1338	10.2983	2.6775	3.0257	2.3700
10	8.98	1.88	2.0188	1.5607	2.1869	6.3051	10.6251	2.4389	2.7509	2.3729
11	8.98	1.88	2.0188	1.5607	2.1869	6.3051	10.6251	2.4389	2.7509	2.3729
$B'$	3.60	4.00	4.3045	3.0917	4.3475	13.662	23.0839	4.8167	5.4259	5.0435
$C'$	10.00	3.00	3.2513	2.9011	4.0231	9.3470	15.6341	4.5753	5.181	3.7082

The dimensions of the corridors are shown in Table 3. The occupants exit the hall using the available source corridors 1–11. Each source corridor has its door denoted as  $A$  to  $I$ . The occupants use the doors to enter the source corridors and then travel to the downstream corridors. They then exit the hall either through an exit door  $A'$  or exit corridors through  $B'$  and  $C'$ .

## 4.2. The performance of the hall utilizing all available routes

Table 3 presents also the optimal arrival rates to each available corridor using the considered speed-density models. Each of the optimal arrival rates generates the optimal throughput with the smallest blocking probability.

**Table 4.** The network flow model for the hall using the Greenshields model

Maximize $x_{T \rightarrow S}$	
!flow out of a super source node equals to its flow in;	
$x_{T \rightarrow S} = x_{s \rightarrow 1} + x_{s \rightarrow 3} + x_{s \rightarrow 5} + x_{s \rightarrow 6} + x_{s \rightarrow 7} + x_{s \rightarrow 8} + x_{s \rightarrow 9} + x_{s \rightarrow 10} + x_{s \rightarrow 11}$	
!flow out of each node equals its flow in; $x_{S \rightarrow 1} = x_{1 \rightarrow 2}$	
$x_{1 \rightarrow 2} = x_{2 \rightarrow 3}$	
$x_{s \rightarrow 3} + x_{2 \rightarrow 3} = x_{3 \rightarrow 4}$	
$x_{3 \rightarrow 4} = x_{4 \rightarrow 5}$	
$x_{S \rightarrow 5} + x_{4 \rightarrow 5} = x_{5 \rightarrow T}$	
$x_{S \rightarrow 6} = x_{6 \rightarrow BBar}$	
$x_{S \rightarrow 7} + x_{8 \rightarrow 7} = x_{7 \rightarrow BBar}$	
$x_{S \rightarrow 8} = x_{8 \rightarrow 7}$	
$x_{S \rightarrow 9} = x_{9 \rightarrow 10}$	
$x_{S \rightarrow 10} + x_{9 \rightarrow 10} = x_{10 \rightarrow CBar}$	
$x_{S \rightarrow 11} = x_{11 \rightarrow CBar}$	
$x_{6 \rightarrow BBar} + x_{7 \rightarrow BBar} = x_{BBar \rightarrow T}$	
$x_{11 \rightarrow CBar} + x_{10 \rightarrow CBar} = x_{CBar \rightarrow T}$	
!flow out of a super sink node equals its flow in; $x_{5 \rightarrow T} + x_{BBar \rightarrow T} + x_{CBar \rightarrow T} = x_{T \rightarrow S}$	
$x_{S \rightarrow 1} \leq 1.3897$	
$x_{1 \rightarrow 2} \leq 1.0754$	
$x_{S \rightarrow 3} + x_{2 \rightarrow 3} \leq 3.1746$	
$x_{3 \rightarrow 4} \leq 1.0754$	
$x_{S \rightarrow 5} + x_{4 \rightarrow 5} \leq 3.4274$	
$x_{S \rightarrow 6} \leq 1.5607$	
$x_{S \rightarrow 7} + x_{8 \rightarrow 7} \leq 1.5607$	
$x_{S \rightarrow 8} \leq 1.7057$	
$x_{S \rightarrow 9} \leq 1.7057$	
$x_{S \rightarrow 10} + x_{9 \rightarrow 10} \leq 1.5607$	
$x_{S \rightarrow 11} \leq 1.5607$	
$x_{6 \rightarrow BBar} + x_{7 \rightarrow BBar} \leq 3.0917$	
$x_{11 \rightarrow CBar} + x_{10 \rightarrow CBar} \leq 2.9011$	

**Table 5.** The performance of the topological network using the Greenshields model

Corridor	$\lambda$	$\theta$	Blocking	$E(N)$	$E(T)$
1	0.0000	0.0000	0.0000	0.0000	0.0000
2	0.0000	0.0000	0.0000	0.0000	0.0000
3	0.0000	0.0000	0.0000	0.0000	0.0000
4	0.0000	0.0000	0.0000	0.0000	0.0000
5	3.4274	3.3898	0.0110	15.7371	4.6424
6	1.5607	1.5396	0.0135	11.8907	7.7231
7	1.5310	1.5260	0.0033	10.8898	7.1363
8	1.5310	1.5310	0.0000	13.6200	8.8962
9	1.5607	1.5607	0.0000	13.9306	8.9259
10	1.5607	1.5396	0.0135	11.8905	7.7230
11	1.3404	1.3404	0.0000	9.1273	6.8094
B'	3.0656	3.0372	0.0093	9.0854	2.9913
C'	2.8800	2.8710	0.0031	23.2745	8.1068
Total throughput of the network: 9.2981 peds/s					

How the optimal arrival rates were used in a network flow model to optimize the flow in the hall based on the Greenshields model is shown in Table 4. Solving the network flow model using any optimization modelling tools, e.g., Lingo (<https://www.lindo.com/>), will generate the optimal arrival rates to source corridors. In this case, Lingo reported that for the Greenshields model,  $\lambda_{S \rightarrow 5} = 3.4274$ ,  $\lambda_{S \rightarrow 6} = 1.5607$ ,  $\lambda_{S \rightarrow 7}$  or  $\lambda_{S \rightarrow 8} = 1.5310$ ,  $\lambda_{S \rightarrow 9}$  or  $\lambda_{S \rightarrow 10} = 1.5607$ ,  $\lambda_{S \rightarrow 11} = 1.3403$  (Table 5) would optimize the flow in the hall. The generated optimal rate was then used to measure their impact on the whole network. The performance of the whole network based on the Greenshields model is presented in Table 5. Notice that the final throughput of the network was calculated based on the total throughput of  $A'$ ,  $B'$  and  $C'$ . Thus, the throughput based on the Greenshields model was  $3.3898 + 3.0372 + 2.8710 = 9.2981$  peds/s.

Table 6 shows the strategies to optimize the throughput of the hall using various speed-density models. The throughputs are sorted from lower to higher values. As observed, the speed-density models generated their own optimized throughputs. The lowest throughput was 9.2981 peds/s, while the highest throughput was 47.5782 peds/s generated by the Greenshields and Drake models, respectively. Compared to the other models, the Greenshields model generated the lowest overall throughput since it generated the lowest optimal arrival rate for each available corridor (see Figure 5 and Table 2) whose values were then used in the network flow model to find the optimal flow in the hall. For the same reason, the Drake model generated the highest throughput since it generated the highest optimal arrival rate value for each corridor. The second lowest throughput (11.2493 peds/s) was generated by the  $M/G/C/C$  exponential model. This model suggests that the occupants should exit the hall using corridor 5 with  $\lambda_{S \rightarrow 5} = 4.1237$ , corridor 6 with  $\lambda_{S \rightarrow 6} = 2.0188$ , corridor 7 with  $\lambda_{S \rightarrow 7} = 2.0188$ , corridor 10 with  $\lambda_{S \rightarrow 10} = 2.0188$  and corridor 11 with  $\lambda_{S \rightarrow 11} = 1.2325$  to optimize the flow in the hall.

**Table 6.** The strategies to optimize the throughput using various speed-density models

Model	Strategy	Total $\theta$	Total $\theta^1$
Greenshields	$\lambda_{S \rightarrow 5} = 3.4274$ , $\lambda_{S \rightarrow 6} = 1.5607$ , $\lambda_{S \rightarrow 7}$ or $\lambda_{S \rightarrow 8} = 1.5310$ , $\lambda_{S \rightarrow 9}$ or $\lambda_{S \rightarrow 10} = 1.5607$ , $\lambda_{S \rightarrow 11} = 1.3403$	9.2981	3.0000
$M/G/C/C$ exponential	$\lambda_{S \rightarrow 5} = 4.1237$ , $\lambda_{S \rightarrow 6} = 2.0188$ , $\lambda_{S \rightarrow 7}$ or $\lambda_{S \rightarrow 8} = 2.0188$ , $\lambda_{S \rightarrow 9}$ or $\lambda_{S \rightarrow 10} = 2.0188$ , $\lambda_{S \rightarrow 11} = 1.2325$	11.2493	8.3809
Greenberg	$\lambda_{S \rightarrow 5} = 4.7818$ , $\lambda_{S \rightarrow 6} = 2.1869$ , $\lambda_{S \rightarrow 7}$ or $\lambda_{S \rightarrow 8} = 2.1606$ , $\lambda_{S \rightarrow 9}$ or $\lambda_{S \rightarrow 10} = 2.1869$ , $\lambda_{S \rightarrow 11} = 1.8362$	12.9932	7.0002
$M/G/C/C$ linear	$\lambda_{S \rightarrow 5} = 4.818$ , $\lambda_{S \rightarrow 6} = 2.3729$ , $\lambda_{S \rightarrow 7}$ or $\lambda_{S \rightarrow 8} = 2.3729$ , $\lambda_{S \rightarrow 9}$ or $\lambda_{S \rightarrow 10} = 2.3729$ , $\lambda_{S \rightarrow 11} = 1.3353$	13.0965	8.9962 [h]
Pipes–Munjaj ( $n = 2$ )	$\lambda_{S \rightarrow 5} = 5.3767$ , $\lambda_{S \rightarrow 6} = 2.4389$ , $\lambda_{S \rightarrow 7}$ or $\lambda_{S \rightarrow 8} = 2.3778$ , $\lambda_{S \rightarrow 9}$ or $\lambda_{S \rightarrow 10} = 2.4389$ , $\lambda_{S \rightarrow 11} = 2.1364$	14.5664	7.0333
Drew ( $n = 1$ )	$\lambda_{S \rightarrow 5} = 6.0745$ , $\lambda_{S \rightarrow 6} = 2.7509$ , $\lambda_{S \rightarrow 7}$ or $\lambda_{S \rightarrow 8} = 2.675$ , $\lambda_{S \rightarrow 9}$ or $\lambda_{S \rightarrow 10} = 2.7509$ , $\lambda_{S \rightarrow 11} = 2.4301$	16.4476	8.4026
Underwood	$\lambda_{S \rightarrow 5} = 12.5132$ , $\lambda_{S \rightarrow 6} = 6.3051$ , $\lambda_{S \rightarrow 7}$ or $\lambda_{S \rightarrow 8} = 6.3051$ , $\lambda_{S \rightarrow 9}$ or $\lambda_{S \rightarrow 10} = 6.3051$ , $\lambda_{S \rightarrow 11} = 3.0419$	28.9877	9.0000
Drake	$\lambda_{S \rightarrow 5} = 21.0195$ , $\lambda_{S \rightarrow 6} = 10.6251$ , $\lambda_{S \rightarrow 7}$ or $\lambda_{S \rightarrow 8} = 10.6251$ , $\lambda_{S \rightarrow 9}$ or $\lambda_{S \rightarrow 10} = 10.6251$ , $\lambda_{S \rightarrow 11} = 5.009$	47.5782	9.0000

<sup>1</sup> Arrival rates to all source corridors set to 1.

Table 6 also shows the performance of the hall if the arrival rates to all source corridors were set to 1, i.e.,  $\lambda_{S \rightarrow 1} = \lambda_{S \rightarrow 3} = \lambda_{S \rightarrow 5} = \lambda_{S \rightarrow 6} = \lambda_{S \rightarrow 7} = \lambda_{S \rightarrow 8} = \lambda_{S \rightarrow 9} = \lambda_{S \rightarrow 10} = \lambda_{S \rightarrow 11} = 1$ . As observed,

this strategy generated much smaller throughputs compared to their optimized strategies in all the speed-density models. For example, this strategy only generated 7.0002 peds/s compared to the optimized strategy which could generate 12.9932 peds/s in the Greenberg model.

### 4.3. The performance of the hall utilizing only a single route

The performance of the hall can also be analyzed if the occupants are forced to only use a single exit route to exit the hall. As mentioned earlier, there are three exit corridors. Thus, three strategies are available to flow out the occupants. Using the data on the corridor dimensions in Table 3, the shortest route is through exit  $A'$  (5.48 m), followed by  $C'$  (11.88 m) and  $B'$  (12.58 m). For more complex topologies, the shortest route [23, 28] can be retrieved using:

$$\min Z = \sum_i \sum_j c_{i \rightarrow j} x_{i \rightarrow j}$$

subject to

$$\sum_j x_{i \rightarrow j} - \sum_k x_{k \rightarrow i} = \begin{cases} 1 & \text{if } i = S \\ -1 & \text{if } i = T, \\ 0 & \text{otherwise} \end{cases} \quad x_{i \rightarrow j} \geq 0$$

where  $c_{i \rightarrow j}$  is the distance from node  $i$  to node  $j$   $x_{i \rightarrow j}$  equal to the flow from node  $i$  to node  $j$ .

**Table 7.** The strategies to optimize the throughput using a single exit

Model	Only exit through $A'$		Only exit through $B'$		Only exit through $C'$	
	Strategy	$\theta$	Strategy	$\theta$	Strategy	$\theta$
Greenshields	$\lambda_{S \rightarrow 5} = 3.4274$	3.3898	$\lambda_{S \rightarrow 6} = 1.5607,$ $\lambda_{S \rightarrow 7} = 1.5310$	3.0372	$\lambda_{S \rightarrow 10} = 1.5607,$ $\lambda_{S \rightarrow 11} = 1.3404$	2.8710
<i>M/G/C/C</i> exponential	$\lambda_{S \rightarrow 5} = 4.1237$	4.0704	$\lambda_{S \rightarrow 6} = 2.0188,$ $\lambda_{S \rightarrow 7} = 2.0188$	3.97015	$\lambda_{S \rightarrow 10} = 2.0188,$ $\lambda_{S \rightarrow 11} = 1.2325$	3.2088
Greenberg	$\lambda_{S \rightarrow 5} = 4.7818$	4.7337	$\lambda_{S \rightarrow 6} = 2.1869,$ $\lambda_{S \rightarrow 7} = 2.1606$	4.2747	$\lambda_{S \rightarrow 10} = 2.1869,$ $\lambda_{S \rightarrow 11} = 1.8362$	3.9847
<i>M/G/C/C</i> linear	$\lambda_{S \rightarrow 5} = 4.8180$	4.7603	$\lambda_{S \rightarrow 6} = 2.3729,$ $\lambda_{S \rightarrow 7} = 2.3729$	4.6735	$\lambda_{S \rightarrow 10} = 2.3729,$ $\lambda_{S \rightarrow 11} = 1.3353$	3.6627
Pipes–Munjaj ( $n = 2$ )	$\lambda_{S \rightarrow 5} = 5.3767$	5.3138	$\lambda_{S \rightarrow 6} = 2.4389,$ $\lambda_{S \rightarrow 7} = 2.3778$	4.7279	$\lambda_{S \rightarrow 10} = 2.4389,$ $\lambda_{S \rightarrow 11} = 2.1364$	4.5247
Drew ( $n = 1$ )	$\lambda_{S \rightarrow 5} = 6.0745$	6.0015	$\lambda_{S \rightarrow 6} = 2.7509,$ $\lambda_{S \rightarrow 7} = 2.6750$	5.3239	$\lambda_{S \rightarrow 10} = 2.7509,$ $\lambda_{S \rightarrow 11} = 2.4301$	5.1222
Underwood	$\lambda_{S \rightarrow 5} = 12.5132$	10.6409	$\lambda_{S \rightarrow 6} = 6.3051,$ $\lambda_{S \rightarrow 7} = 1.3403$	6.3051	$\lambda_{S \rightarrow 10} = 6.3051,$ $\lambda_{S \rightarrow 11} = 3.0419$	8.0760
Drake	$\lambda_{S \rightarrow 5} = 21.0195$	17.5202	$\lambda_{S \rightarrow 6} = 10.6251,$ $\lambda_{S \rightarrow 7} = 10.6251$	16.8160	$\lambda_{S \rightarrow 10} = 10.6251,$ $\lambda_{S \rightarrow 11} = 5.009$	13.2420

Table 7 shows the strategies to optimize the throughput of the hall using a single exit route. Exit route  $A'$  should be used to flow the occupants since it generates better throughputs compared to other exit routes in all speed-density models. For example, the *M/G/C/C* exponential model recommends that the occupants should have flowed with 4.1237 peds/s to achieve the optimal throughput of 4.0704 peds/s. However, for all speed-density models, this strategy produces a much smaller throughput compared to

flowing the occupants using all available routes.

#### 4.4. The best model for optimising pedestrian flow in a topological network

This paper considers and compares seven different speed-density models for optimising pedestrian flow in a topological network. The question is which model is the best for the purpose. To answer this question, we should evaluate the density of occupants/pedestrians in a considered facility or topological network. If the facility/topological network has a high density of occupants/pedestrians, models that predict speed at a higher density should be used. Examples are the Greenshields, *M/G/C/C*, Greenberg, Pipes–Munjal and Drew models. Under this situation, the Underwood and Drake models are ineffective since neither can correctly predict speed at a high density. If the facility/topological network has a low number of occupants/pedestrians, models that predict speed at a lower density should be employed. Examples are Greenshields, Pipes–Munjal and Drew, Underwood and Drake models. In this case, the *M/G/C/C* and Greenberg models are unsuitable. Since the network flow model attempts to derive the optimal density in each available network, the Greenshields, Pipe–Munjal and Drew models are the best models for optimising pedestrian movement across a topological network.

### 5. The limitations of the study

This study has two main limitations. The first limitation is that this study only examined the interaction between speed and crowd density under a normal or typical situation. Under this condition, the optimal arrival rates to source networks were then derived to maximise the flow across a topological network. In emergency situations, such simulations and evaluations may be inaccurate since pedestrian behavior is unpredictable and complex to model. The behavior (such as panic, confusion and stampede) will slow down pedestrian movement which may result in a reduction in overall throughput.

The second limitation is that our methodology is primarily concerned with determining the optimal arrival rates to the source networks under a stability condition, in which the network flow is smooth with little blocking to ensure that pedestrians do not overflow in each available network. It is not intended to be used to analyse arrival rates that are higher than the optimal arrival rates, since this may cause the networks to explode and cause blocking in downstream networks.

### 6. Conclusion

Pedestrians' speed and flow in a network, affected by their density, can be calculated using speed-density models. The models can additionally be utilised to optimally control pedestrians' density by regulating their arrival rates. This paper optimises the arrival rates to the source networks of a topological network and analyses their effects on the performance of each available network using the speed-density models and network flow program. The results show that the optimal arrival rates generate the smoothest flow in the whole network and maximises its throughput.

The analysis can help decision-makers get insight into how to manage traffic flow in public facilities and building networks. In whatever cases, flowing pedestrians out of a facility using a single shortest



route would not produce good throughput as flowing pedestrians using all available routes. To help decision-makers visualise the pedestrians' real behaviour, it is recommended that future research can animate the pedestrians' movement in the topological network based on the optimised strategy and other considered strategies using simulation tools.

## Acknowledgement

This research was supported by the Ministry of Higher Education (MoHE) of Malaysia through the Fundamental Research Grant Scheme (FRGS/1/2019/STG06/UUM/03/1). We wish to thank the Ministry of Higher Education (MoHE) of Malaysia and Universiti Utara Malaysia for the financial support. The funder had no role in study design, data collection and analysis, decision to publish or preparation of the manuscript. The authors are grateful to the anonymous reviewers for their valuable comments and suggestions made on the previous draft of this manuscript.

## References

- [1] BRADLEY, S. P., HAX, A. C., AND MAGNANTI T. L. *Applied Mathematical Programming*. Addison-Wesley Publishing Company, Boston, 1977.
- [2] CHEAH, J., AND MACGREGOR SMITH, J. Generalized M/G/C/C state dependent queueing models and pedestrian traffic flows. *Queueing Systems* 15, 1 (1994), 365–386.
- [3] DAHIYA, G., ASAKURA, Y., AND NAKANISHI, W. Analysis of the single-regime speed-density fundamental relationships for varying spatiotemporal resolution using Zen Traffic Data. *Asian Transport Studies* 8 (2022), 100066.
- [4] DRAKE, J. S., SCHOEFER, J. L., AND MAY, A. D. A statistical analysis of speed density hypothesis. *Highway Research Record* 154 (1965), 53–87.
- [5] DREW, D. R. *Traffic Flow Theory and Control*. McGraw-Hill, New York, 1968.
- [6] EDIE, L. C. Car-following and steady-state theory for noncongested traffic. *Operations Research* 9, 1 (1961), 66–76.
- [7] FRUIN, J. J. *Pedestrian Planning and Design*. Metropolitan Association of Urban Designers and Environmental Planners, New York, 1971.
- [8] GREENBERG, H. An analysis of traffic flow. *Operations Research* 7, 1 (1959), 79–85.
- [9] GREENSHIELDS, B. D., BIBBINS J. R., CHANNING W. S., MILLER H. H. A study of traffic capacity. *Highway Research Board Proceedings* 14 (1935), 448–477.
- [10] HANKIN, B. D., AND WRIGHT, R. A. Passenger flow in subways. *Operational Research Quarterly* 9, 2 (1958), 81–88.
- [11] HILLIER, F. S., AND LIEBERMAN, G. J. *Introduction to Operations Research*. McGraw-Hill, New York, 2001.
- [12] JING, W.-L. *Introduction to Network Traffic Flow Theory: Principles, Concepts, Models, and Methods*. Elsevier, Amsterdam, 2021.
- [13] KHALID, R., BATEN, M. A., NAWAWI, M. K. M., AND ISHAK, N. Analyzing and optimizing pedestrian flow through a topological network based on M/G/C/C and network flow approaches. *Journal of Advanced Transportation* 50, 1 (2016), 96–119.
- [14] KHALID, R., NAWAWI, M. K. M., KAWSAR, L. A., GHANI, N. A., KAMIL, A. A., AND MUSTAFA, A. A discrete event simulation model for evaluating the performances of an M/G/C/C state dependent queueing system. *PLoS ONE* 8, 4 (2013), e58402.
- [15] KHALID, R., NAWAWI, M. K. M., KAWSAR, L. A., GHANI, N. A., KAMIL, A. A., AND MUSTAFA, A. The evaluation of pedestrians' behavior using M/G/C/C analytical, weighted distance and real distance simulation models. *Discrete Event Dynamic Systems* 26, 3 (2016), 439–476.
- [16] KHALID, R., NAWAWI, M. K. M., KAWSAR, L. A., GHANI, N. A., KAMIL, A. A., AND MUSTAFA, A. Optimal routing of pedestrian flow in a complex topological network with multiple entrances and exits 51, 8 (2020), 1325–1352.
- [17] MAY, A. D. *Traffic Flow Fundamentals*. Prentice Hall, Englewood Cliffs, NJ, 1990.
- [18] NAVIN, F. P., AND WHEELER, R. J. Pedestrian flow characteristics. *Traffic Engineering* 39 (1969), 31–36.
- [19] OEDING, D. Traffic loads and dimensions of walkways and other pedestrian circulation facilities. *Straßenbau und Straßenverkehrstechnik* 22 (1963), 160–163.
- [20] OLDER, S. J. Movement of pedestrians on footways in shopping streets. *Traffic Engineering and Control* 10, 4 (1968), 160–163.
- [21] PIPES, L. A. Car following models and the fundamental diagram of road traffic. *Transportation Research* 1 (1967), 21–29.
- [22] PREDTECHENSKII, V. M., AND MILINSKII, A. I. *Planning for Foot Traffic Flow in Buildings*. Amerind Publishing, New Delhi, 1983.
- [23] RENDER, B., STAIR, R. M., HANNA, M. E., AND HALE, T. S. *Quantitative Analysis for Management*. Pearson, London, 2015.
- [24] SMITH, J. M. *Evacuation Networks*. In *Encyclopedia of Optimization*, C. A. Floudas and P. M. Pardalos, Eds., Kluwer Academic Publishers, Dordrecht, 2001, pp. 576–584.
- [25] SMITH, J. M., AND CRUZ, F. R. B. M/G/c/c state dependent travel time models and properties. *Physica A: Statistical Mechanics and its Applications* 395, (2014), 560–579.

- 
- [26] STEWART, J. *Multivariable Calculus*. Brooks/Cole Cengage Learning, Belmont, 2012.
- [27] SUN, L., GONG, Q., YAO, L., LUO, W., AND ZHANG, T. A dynamic time warping algorithm based analysis of pedestrian shockwaves at bottleneck. *Journal of Advanced Transportation 2018* (2018), 1269439.
- [28] TAYLOR III, B. W. *Introduction to Management Science*. Pearson, London, 2016.
- [29] UNDERWOOD, R. T. *Speed, Volume and Density Relationships*. Bureau of Highway Traffic, Yale University, Victoria 1960.
- [30] WEISS, A., WILLIAMS, L., AND SMITH, J. M. Performance & optimization of M/G /c/c building evacuation networks. *Journal of Mathematical Modelling and Algorithms 11*, 4 (2012), 361–386.
- [31] WINSTON, W. L. *Operations Research. Applications and Algorithms*. Cengage Learning, Boston 2004.
- [32] WINSTON, W. L., AND ALBRIGHT, S. C. *Practical Management Science*. Cengage Learning, Boston, 2019.
- [33] YU, C., ZHANG, J., YAO, D., ZHANG, R., AND JIN, H. Speed-density model of interrupted traffic flow based on coil data. *Mobile Information Systems 2016* (2016), 7968108.
- [34] YUHASKI JR, S. J., AND SMITH, J. M. Modeling circulation systems in buildings using state dependent queueing models. *Queueing Systems 4*, 4 (1989), 319–338.